Temperature and pH Dependence XAFS Study of $Gd(DOTA)^-$ and $Gd(DTPA)^{2-}$ Complexes: Solid State and Solution Structures

Simone Bénazeth,*[,†,‡] Juris Purans,[†,§] Marie-Cécile Chalbot,[†,‡] M. Kim Nguyen-van-Duong,[||] Louisette Nicolas,[||] Françoise Keller,[⊥] and Alain Gaudemer[||]

Laboratoire de Chimie Inorganique, UFR Pharmacie, Université Paris XI, 92296 Paris, France, LURE, Bat 209D, Université Paris XI, 91405 Orsay, France, Laboratoire de Chimie Bioorganique et Bioinorganique, Bat 420, Université Paris XI, 91405 Orsay, France, Laboratoire de Physique-biomathématiques, Faculté de pharmacie, Université Paris V, 75006 Paris, France, and Institute of Solid State Physics, University of Latvia, Kengaraga 8, 1063 Riga, Latvia

Received June 12, 1997

We present an X-ray absorption spectroscopy study of the local structures of $Gd(DTPA)^{2-}$ and $Gd(DOTA)^-$ complexes in the crystalline state (at room and low temperatures) and in aqueous solutions exhibiting various pH values (0.15−7) at different temperatures (25−90 °C). Using X-ray absorption fine structure (XAFS) analysis procedures and ab initio multiple scattering calculations of XAFS spectra at the Gd L_3 edge, we reconstructed the Gd^{3+} local environment, and compared it with existing structural models. From neutral pH to a value of 1.5, we found that the local environment and complex dynamics around the gadolinium ions were conserved up to 4.5 Å, and the structure agreed well with the known crystallographic data. In these solutions, the gadolinium ions in the complex $Gd(DOTA)^-$ are bonded to the four carboxylate oxygen atoms [R(Gd−O_{av}) 2.38 Å, Debye−Waller (DW) factor 0.006 Å^2], to the four nitrogen atoms [R(Gd−N_{av}) 2.65 Å, DW factor 0.006 Å^2] and to one water molecule [R(Gd−O_w) 2.46 Å, DW factor 0.012 Å^2]. Concerning the complex $Gd(DTPA)^{2-}$, the gadolinium ions are bonded to the five carbonyl oxygen atoms [R(Gd−O_{av}) 2.39 Å, DW factor 0.007 Å^2], to the three nitrogen atoms [R(Gd−N_{av}) 2.64 Å, DW factor 0.006 Å^2], and to one water molecule [R(Gd−O_w) 2.47 Å, DW factor 0.018 Å^2]. In the range of pH (0.15−1.5) for the $Gd(DTPA)^{2-}$ complexes, thanks to the pH strong dependence of the XAFS signals, we observed a progressive complex dissociation. On the other hand, the XAFS signals of $Gd(DOTA)^-$ complexes exhibited only a slight pH (1−1.5) dependence. Concerning both complexes, we noted just a slight temperature dependence.

Introduction

In recent years magnetic resonance imaging (MRI) has become an important diagnostic method in medicine. The lanthanide compounds and, more specifically, the Gd^{3+} complexes are some of the various paramagnetic contrast agents.[1−7] The ligands of the Gd^{3+} complexes are commonly macrocycles, as, for instance, DOTA (1,4,7,10-tetraazacyclododecane-1,4,7,10-tetraacetic acid) in the complex $Gd(DOTA)^-$ and DTPA (diethylenetriaminopentaacetic acid) in the complex $Gd(DTPA)^{2-}$ (Figure 1: complex schemes).[1−3] The rate of formation and equilibrium constant for the outer-sphere complex formation have been widely studied.[3−7] Numerous structural studies have been devoted to these complexes in order to approach the factors which determine the proton relaxivity. However, the questions concerning the structures of the aqueous solutions as well as the influence of some external factors [temperature, pH, presence of other potential rare-earth cation ligands (proteins)] on the gadolinium coordination sphere have not yet been resolved.

Deduced from X-ray diffraction analysis,[8,9] the surrounding of the nine-coordinated Gd^{3+} ion in $[Gd(DOTA)H_2O]^-$ is known in the crystalline state. This cation is inside the macrocycle and bound to four carboxylate oxygen atoms (2.36−2.37 Å) with an average distance (Gd−O_{av}) of 2.36 Å, four nitrogen atoms (2.65−2.68 Å) with an average distance (Gd−N_{av}) of 2.66 Å, and one inner-sphere water molecule (2.45 Å). The coordination geometry is a distorted capped square antiprism. Conversely, in the complex $Gd(DTPA)^{2-}$, the nine-coordinated Gd^{3+} ion is bound to five carboxylic oxygen atoms from the acetate groups (2.36−2.44 Å) with an average distance of 2.40 Å, to three amino nitrogen atoms (2.58−2.71 Å) with an average distance of 2.64 Å, and to one water molecule (2.49 Å).[10,11] The coordination geometry is a distorted capped square antiprism, also.

† Laboratoire de Chimie Inorganique, Université Paris XI.
‡ LURE, Université Paris XI.
§ University of Latvia.
|| Laboratoire de Chimie Bioorganique et Bioinorganique, Université Paris XI.
⊥ Université Paris V.

(1) Weinmann, H. J.; Brasch, R. C.; Press: W. R.; Wesbey, G. E. *Am. J. Roentgenol.* **1984**, *142*, 619.
(2) Ubersicht, E.; Felix, V. R.; Semmler, W.; Schorner, W.; Laniado, M. *Fortschr. Roentgenstr.* **1985**, *142*, 641.
(3) Loncin, M. F.; Desreux, J. F.; Merciny, E. *Inorg. Chem.* **1986**, *25*, 2646.
(4) Lauffer, R. B. *Chem. Rev.* **1987**, *87*, 901.
(5) Chaubet, F.; Nguyen-van-Duong, K.; Courtieu, J.; Gaudemer, A.; Greff, A.; Crumbliss, A. L. *Can. J. Chem.* **1991**, *69*, 1107.
(6) Aime, S.; Botta, M.; Ermondi, G. *Inorg. Chem.* **1992**, *31*, 4291.
(7) Aime, S.; Botta, M.; Fasano, M.; Geninatti, S.; Terreno, E. *J. Biol. Inorg. Chem.* **1996**, *1*, 312.
(8) Dubost, J. P.; Leger, J. M.; Langlois, M. H.; Meyer, D.; Schaefer, M. *C. R. Acad. Sci., Ser. II* **1991**, *312*, 349.
(9) Chang, C. A.; Francesconi, L. C.; Malley, M. F.; Kumar, K.; Gougoutas, J. Z.; Tweedle, M. F. *Inorg. Chem.* **1993**, *32*, 3501.

S0020-1669(97)00732-5 CCC: $15.00
Published on Web 06/24/1998

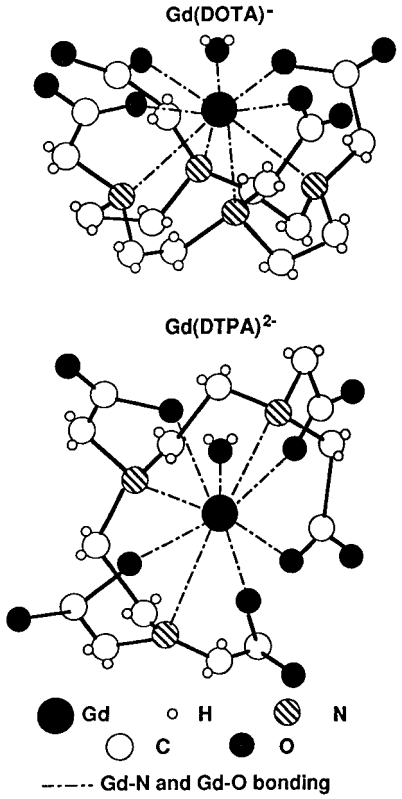

Figure 1. $Gd(DOTA)^-$ and $Gd(DTPA)^{2-}$ complex schemes.

A detailed NMR structural study was published on the aqueous solutions of rare-earth DOTA complexes,[6] which suggests that the dynamic process occurs through successive changes in conformations of ethylenic groups and that the rigidity of the macrocycle ring evolves as the temperature increases. Concerning the DTPA complexes, a two-dimensional NMR analysis was performed on the aqueous solutions and the authors concluded [6,12] that there were two enantiomeric forms in which coordinated terminal acetates are exchanged. Moreover, in solutions, the NMRD profiles suggest that the next nearest water molecule is 4.25 Å distant from Gd.[13]

The pH dependence relaxivity NMR and luminescence studies for both complexes show a tendency to dissociation in the low-pH range. It must be noted that the small paramagnetic shifts and the large peak widths induced by these Gd complexes render useless their study by NMR spectroscopy.[15] However, a kinetics study on the DOTA complex was carried out by scavenging the liberated $^{153}Gd^{3+}$ with an ion exchanger. It showed an exceedingly slow dissociation even in acidic solution (pH 2−4) which lasts a few days. The $Gd(DOTA)^-$ complex appeared to be the most stable lanthanide complex, due to its very low rates of dissociation.[15] However, the thermodynamic stability of $Gd(DOTA)^-$ is comparable to that of $Gd(DTPA)^{2-}$. In acidic media (pH 2 and lower), the negatively charged complexes can be protonated, and the acid-assisted dissociation mechanism was proposed.[16]

In this paper, we present an X-ray absorption fine structure (XAFS) study on $Gd(DOTA)^-$ and $Gd(DTPA)^{2-}$ complexes, in the crystalline state and aqueous solutions for various pH values (0.15−7) at room temperature and for various temperatures (25−90 °C) at pH 1.5. An additional study of $GdCl_3$ (0.2 M aqueous solution as a reference solution) was carried out at the Gd L_3 edge to understand the hydration of the Gd^{3+} ions. Moreover, the multiple scattering analyses of XAFS signals up to 5 Å have also been carried out. This spectroscopy was chosen because it is indeed a technique well suited to provide direct structural information on a cluster core geometry in both states up to 5 Å, while the X-ray diffraction technique mainly gives information about the crystal structure.

XAFS experiments have previously shown that many transition metal[18,19] and uranium macrocyclic complexes[20] in solutions conserved the first coordination shell of the metal (i.e., the first peak in the FT), whereas the next peaks in the FT associated with the next shells of the metal in the macrocycle did not. To cancel important macrocyclic signatures and to reveal residual signals, Goulon et al.[19] developed perturbed difference analyses of XAFS and detected considerable multiple scattering (MS) effects beyond the first shell in porphyrinic complexes.

As far as we know, no comparative XAFS studies on rare-earth metal macrocyclic complexes have ever been reported in the crystalline state and in solutions. Consequently, we carried out our XAFS study on the local environment of the Gd^{3+} ion in an aqueous solution and compared it with the XAFS study on the complexes $Gd(DTPA)^{2-}$ and $Gd(DOTA)^-$ in their various aqueous solutions and solid state forms. The presence of only one water molecule in the first coordination shell of the Gd^{3+} ion in the complexes makes the XAFS analysis particularly delicate. This explains why we provide so many details concerning ab initio MS calculations and criteria to optimize the calculated amplitude and phase functions of the backscattering atoms.

Experimental Section

Chemicals and Solutions. The $Gd(DTPA)^{2-}$ and $Gd(DOTA)^-$ complexes were prepared by the reaction of the appropriate ligands with gadolinium oxide in deionized water, and we isolated a white solid after lyophilization.[21] The XAFS and IR studies were performed with the (0.2 M) solutions that were obtained by dissolving the solid forms of the complexes in water. Then the pH was adjusted up to 9 with NaOH or down to 0.15 with concentrated HCl. The aqueous

(10) Gries, H.; Miklautz, H. *Physiol. Chem. Phys. Med. NMR* **1984**, *16*, 105.
(11) Stezowski, J. J.; Hoard, I. L. *Isr. J. Chem.* **1984**, *24*, 323.
(12) Jenkins, B. G.; Lauffer, R. B. *Inorg. Chem.* **1988**, *27*, 4730. Jenkins, B. G.; Armstrong, B. J.; Lauffer, R. B. *Magn. Reson. Med.* **1991**, *17*, 164.
(13) Aime, S.; Batsov, A. S.; Botta, M.; Howard, J. A. K.; Parker, D.; Senanayake, K.; Williams, G. *Inorg. Chem.* **1994**, *33*, 4696.
(14) Chang, C. A.; Brittain, H. G.; Tesler, J.; Tweedle, M. F. *Inorg. Chem.* **1990**, *29*, 4468. Zhang, X.; Chang, C. A.; Brittain, H. B.; Garrison, J. M.; Tesler, J.; Tweedle, M. F. *Inorg. Chem.* **1992**, *31*, 5597.
(15) Wang, X.; Jin, T.; Comblin, V.; Lopez-Mut, A.; Merciny, E.; Desreux, J. F. *Inorg. Chem.* **1992**, *31*, 1095.
(16) Kumar, K.; Tweedle, M. F. *Appl. Chem.* **1993**, *65*, 3, 515. Kumar, K.; Jin, T.; Wang, X., Desreux, J. F.; Tweedle, M. F. *Inorg. Chem.* **1994**, *33*, 3823. Kumar, K.; Jin, T.; Chang, C. A.; Tweedle, M. F. *Inorg. Chem.* **1993**, *32*, 587.
(17) Duncan, J. R.; Franano, F. N.; Edwards, W. B.; Welch, M. J. *Invest. Radiol.* **1994**, *29*, 58.
(18) Hasnain, S. S. EXAFS and XANES Studies of Copper Proteins. In *Biophysics and Synchrotron Radiation*; Springer Series in Biophysics, Vol. 2; Bianconi, A., Congiu-Castellano, A., Eds.; Springer-Verlag: Berlin, 1987; p 147.
(19) Goulon, J.; Loos, M.; Ascone, I.; Goulon-Ginet, C.; Battioni, P.; Battioni, J. P.; Mahy, J. P.; Mansuy, D.; Meunier, B. Structural Investigation of Biomimetic Complexes of Cytochrome P-450 by Difference EXAFS Spectroscopy. In *Biophysics and Synchrotron Radiation*; Springer Series in Biophysics, Vol. 2; Bianconi, A., Congiu-Castellano, A., Eds.; Springer-Verlag: Berlin, 1987; p 191. Goulon, J.; Friant, P.; Goulon-Ginet, C.; Coutsolelos, A.; Guilard, P. *Chem. Phys.* **1984**, *83*, 367.
(20) Charpin, P.; Dejean, A.; Folcher, G.; Rigny, P.; Navaza, P. *J. Chem. Phys.* **1985**, *82*, 925.
(21) Griselda, H.; Tweedle, M. F.; Bryant, R. G. *Inorg. Chem.* **1990**, *29*, 5109.

solution samples (0.2 M) were prepared in cells whose thickness varied between 1 and 3 mm. In both cases, we optimized the experimental parameters in order to achieve a jump to the X-ray absorption edge between 0.5 and 1. With infrared spectroscopy experiments, we first determined the acidity conditions of the dissociation of the Gd complexes. We thus observed that $Gd(DOTA)^-$ was not stable at an acidity lower than pH 1.

XAFS Measurements. The XAFS spectra at the Gd L_3 edge were measured in the transmission mode for the aqueous solutions at different temperatures (25−90 °C, pH 1.5) and at different pH values (0.15−7) at room temperature. Moreover, the complexes in the crystalline state were measured at room and low (−193 °C) temperatures. We also registered the XAFS spectra of aqueous solutions of $GdCl_3$ which are known to be totally dissociated at pH 0.3 and pH 7.

X-ray absorption spectra at the Gd L_3 edge were measured in the transmission mode with the DCI D13 (EXAFS-3) beam line (LURE, Orsay, France; ring current 350−250 mA; beam energy 1.85 GeV). The synchrotron radiation was monochromatized using a Si(311) double-crystal monochromator, and 50% of harmonic rejection was achieved by slightly detuning the two crystals from the parallel alignment. The range of the L_3 edge ($E_{L_3} = 7242$ eV) XAFS is limited by the presence of the gadolinium L_2 edge ($E_{L_2} = 7930$ eV). Therefore the experimental spectra were measured by two ionization chambers filled with air in the energy range from 7000 to 7900 eV with the step 1 eV, count rate 2 s per point, and the energy resolution (fwhm) being 2.0 eV (Si(311)). The white line edge positions were reproducible with a precision better than 0.1 eV.

A multipurpose X-ray absorption cell[22] was used for in-situ XAFS measurements of the solutions in the transmission mode under various experimental conditions: temperatures 20−90 °C; pH 0.15−7. The temperature varied within the range from RT to 90 °C and was stabilized within ±2 °C during each measurement. Moreover, the solid state sample for X-ray absorption measurements was prepared from a polycrystalline form whose quality was checked by X-ray powder diffraction. The powder was finely ground and mechanically mixed with cellulose powder. The variations of the XAFS spectra related to the slit width were studied and adjusted to render the spectra well defined for the data analysis. The influence of the sample thickness was studied at different cell path lengths, concentrations, and powder sample thicknesses. Finally, the thickness of the sample permitted us to reach the value of the absorption jump from 0.5 to 1. A total of about 10 scan data (about 4 h) were collected for the solutions, and each spectrum was checked individually before averaging. At high temperatures (80 °C), we observed more noisy experimental spectra due to the instability of the cell.

XAFS Data Analysis. The experimental data were analyzed by applying constraint refinement based on crystallographic data and lattice dynamics. For the known complexes, we had to constrain the parameters in order to obtain integer values of occupation numbers, and the same DW factor for similar types of atoms at similar distances from Gd.[22,23]

Moreover, low-symmetry crystalline complexes such as $Gd(DTPA)^{2-}$ and $Gd(DOTA)^-$ contain many distances in one subshell, and therefore the DW factors obtained have static and dynamic contributions. To circumvent the averaging problem of many contributions in one subshell, after we had ajusted the DW factors, the RDF's were simulated with all the interatomic distances and the coordination numbers obtained from crystallographic (XRD) data. In such a way, the reconstructed RDF's from the XAFS data were compared with those obtained from the crystallographic XRD data. As a result, the structural disorder due to the continuous distribution of distances and the thermal (vibrational) disorder were quantitatively taken into account.

On the other hand, the DW factors of the $Gd(DTPA)^{2-}$ and $Gd(DOTA)^-$ complexes as well as Gd^{3+} ions in solutions can be described as the sum of σ_{stat}^2 due to static disorder, σ_{vib}^2 due to thermal vibrations, and σ_{exch}^2 (only for the water molecules) due to the exchange of water molecules between the first and second hydration shells.[24]

The experimental data were analyzed with the EXAFS data analysis software package EDA[25] implementing the data analysis simple constraint refinement based on crystallographic data and lattice dynamics described above. The X-ray absorption coefficient $\mu(E) = \ln(I_0/I)$ was obtained from the intensities of the synchrotron radiation, measured by two ionization chambers, one before (I_0) and the other (I) after the sample. The background contribution $\mu_b(E)$ was so considerable in solutions that we had to improve the algorithms of the background subtraction.[25,26] At the first step, the background contribution $\mu_b(E)$ was estimated by the Victoreen rule ($\mu_b = A/E^3 + B/E^4$) and subtracted from the experimental spectrum $\mu(E)$. Furthermore, the atomic-like contribution $\mu_0(E)$[27,28] was calculated by a combined polynomial/cubic-spline technique in order to have a precise removal of the XAFS signal zero line. Finally, the XAFS signal $\chi(E)$ was determined as $\chi(E) = (\mu - \mu_b - \mu_0)/\mu_0$.

We converted $\chi(E)$ to the space of the photoelectron wavevector k, defined as $k = [(2m/\hbar^2)(E - E_0)]^{1/2}$, where $(E - E_0)$ is the photoelectron kinetic energy measured from the inner core photoemission threshold (vacuum level). In the case of the L_3 edge of rare-earth elements, it is located behind the white line, which corresponds to the unoccupied 5d states. In the present work, the energy origin E_0 was located at 2 eV above the white line maximum, according to the method we had previously used.[27,28] The experimental XAFS signal $\chi(k)$ was multiplied by a factor k^2 to compensate for the decrease in its amplitude with the increase in the wavevector value (see Figure 2).

Figure 3 shows the Fourier transforms (FT's) of the experimental XAFS signals, with a Kaiser−Bessel window in the range from 1.0 to 13.0 $Å^{-1}$ for $Gd(DOTA)^-$ and $Gd(DTPA)^{2-}$. Modulus and imaginary parts of the FT's are not corrected for the photoelectron phase shift; therefore, the positions of the peaks differ about 0.5 Å from the true crystallographic values. In all the FT's of the experimental spectra (see Figure 3), there is one main peak located at 1.8 Å, a group of peaks from 2.2 to 3.4 Å, and lower peaks from 3.4 to 5 Å. The low intensity of the FT signal above 6 Å indicates that the noise in the experimental spectrum has a "white" character. The absence of any significant contribution near $R = 0$ Å indicates good removal of the μ_0 signal.

We started with the first-shell XAFS signal analysis. The XAFS signals were fitted using standard harmonic two- or three-shells models,[28] in which the distribution of distances (RDF) was taken into account by a superposition of two or three Gaussian distributions:

$$\chi(k) = \sum_{i=1}^{3} (N_i/kR_i^2)\, f(\pi, k, R_i) \exp(-2\sigma_i^2 k^2) \sin(2kR_i + \phi(\pi, k, R_i))$$

In this expression, N_i is the coordination number, R_i is the interatomic distance, σ_i is the DW factor, and k is the photoelectron wavevector. The experimental XAFS signals of the first coordination shell of Gd were singled out by the back FT procedure in the range 0.8−2.6 Å and were used in further analysis. Calculations of the XAFS function were based on the single-scattering curved-wave formalism which is suitable for the first shell.

The backscattering amplitude $f(\pi, k, R)$ and phase $\phi(\pi, k, R)$ functions were calculated using the FEFF6 code[29] for both clusters (GdO_5N_4 (ideal capped square antiprism) and $GdO_5N_4C_{16}$) with the distances Gd−O (R = 2.4 Å), Gd−N (R = 2.7 Å), and Gd−C (R =

(22) Co, M. C.; Hodgson, K. O. *J. Am. Chem. Soc.* **1981**, *103*, 3200.
(23) Binsted, N.; Strange, R. W.; Hasnain, S. S. *Biochemistry* **1992**, *31*, 12117.
(24) Yamaguchi, T.; Nomura, M.; Wakita, H.; Ohtaki, H. *J. Chem. Phys.* **1988**, *89*, 5153.
(25) Kuzmin, A. *Physica B* **1995**, *208*, 40. Kuzmin, A.; Obst, S.; Purans, J.; Benfatto, M.; Natoli, C. R. *J. Phys.: Condens. Matter* **1997**, *9*, 1.
(26) Report on the International Workshop on Standards and Criteria in XAFS. In *X−Ray Absorption Fine Structure*; Hasnain, S. S., Ed.; Ellis Horwood: New York, 1991; p 751.
(27) Kuzmin, A.; Purans, J.; Benfatto, M.; Natoli, C. R. *Phys. Rev.* **1993**, *B47*, 2480.
(28) Rocca, F.; Kuzmin, A.; Purans, J.; Mariotto, G. *Phys. Rev.* **1994**, *B50*, 6662.
(29) Rehr, J. J.; Mustre de Leon, J.; Zabinsky, S. I.; Albers, R. C. *J. Am. Chem. Soc.* **1991**, *113*, 5135−5140.

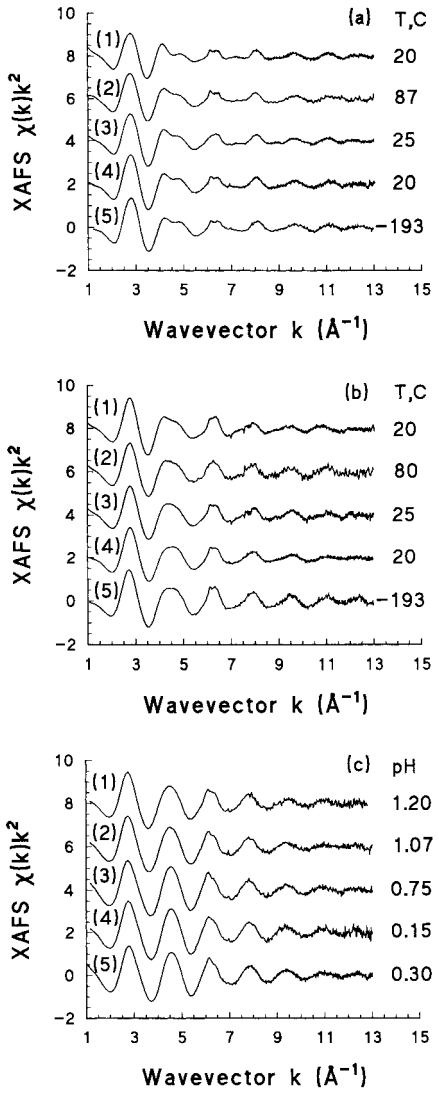

Figure 2. Experimental XAFS spectra $\chi(k)k^2$ of the $Gd(DOTA)^-$ complex (a) and $Gd(DTPA)^{2-}$ complex (b) in the crystals and in the aqueous solutions: (1) pH 7, RT aqueous solution; (2) pH 1.5, 87 °C (DOTA) and 80° (DTPA) aqueous solutions; (3) pH 1.5, 25 °C aqueous solution; (4) RT crystal; (5) LT crystal. Acidification of the $Gd(DTPA)^{2-}$ complex (c) in the aqueous solutions at RT: (1) pH 1.20; (2) pH 1.07; (3) pH 0.75; (4) pH 0.15; (5) Gd^{3+} ion in aqueous solution pH 0.3. All spectra are plotted on the same vertical scale and displaced vertically for clarity.

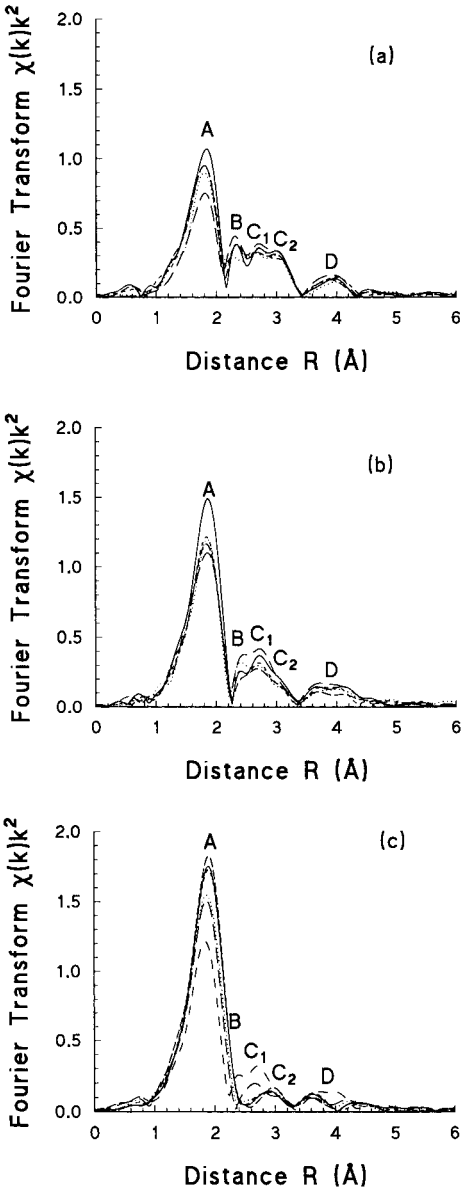

Figure 3. FT's (modulus part) of the experimental XAFS spectra of the $Gd(DOTA)^-$ complex (a) and $Gd(DTPA)^{2-}$ complex (b) in the crystals and in the aqueous solutions (see peak A from up to down): the crystals at LT (full line) and at RT (dashed line); the aqueous solutions at pH 1.5, 25 °C (dotted line) and pH 7, RT (dashed short line). Acidification of the $Gd(DTPA)^{2-}$ complex (c) in the aqueous solutions at RT solutions (see peak A from down to up): pH 1.50 (dashed line—smallest A peak and highest B and C_2 peaks); pH 1.20 (dashed line with long cycle); pH 1.07 (dotted line); pH 0.75 (dashed line with short lines); pH 0.15 (dashed line with long lines); the Gd^{3+} ion in aqueous solution at pH 0.3 (full line) is also shown.

3.2 and 3.5 Å) and the muffin tin radii $R_{mt}(Gd) = 1.43$ Å, $R_{mt}(O) = 0.97$ Å, $R_{mt}(N) = 0.90$ Å, and $R_{mt}(C) = 0.76$ Å. The cluster $GdO_5N_4C_{16}$ presents a greater symmetry and mimics the structure of the $Gd(DOTA)^-$ complex. Additional calculations have been done for the GdO_9 (three capped trigonal prism $R = 2.41$ Å) and GdO_8 (square antiprism $R = 2.41$ Å) clusters, which mimic the possible environment of Gd^{3+} ions in aqueous solutions.[24,29−33]

Since the origin energy E_0 of the photoelectron is defined in the FEFF6 code[29] relative to the Fermi level E_F and strongly depends on the muffin tin radii, we chose the continuum threshold (2 eV above the white line maximum). The amplitude $f(\pi, k, R)$ and phase $\phi(\pi, k, R)$ functions were tested with the experimental XAFS data of Gd^{3+} ions in aqueous solutions. The position of the origin energy E_0 of the photoelectron was fixed as described before. The photoelectron mean-free path contribution was automatically included in the scattering amplitude function using the complex Hedin−Lundqvist (HL) exchange and the correlation potential (ECP). This ECP computation is based on the density functional formalism within the one-plasmon approximation, in the scattering **T**-matrix calculation. A natural broadening was included through the core level width $\Gamma_{core-hole} = 3.5$ eV for the $2p_{3/2}$ level in the case of the Gd L_3 edge.

Gadolinium aqueous solutions (0.2 M and pH 7, 4, 1, and 0.3) obtained from the dissolution of the $GdCl_3$ salt were used to check the theoretical MS calculations and the backscattering amplitude and phase functions for Gd−O atoms pair (see previous XAFS investigations)[24,34] and XAFS results shown in Figure S1 (Supporting Information). Moreover, the accuracy of the theoretical backscattering amplitude and

(30) Cossy, C.; Barnes, A. C.; Enderby, J. E.; Merbach, A. E. *J. Chem. Phys.* **1989**, *90*, 3254.
(31) Cossy, C.; Helm, L.; Powell, D. H.; Merbach, A. E. *New J. Chem.* **1995**, *19*, 27.
(32) Kowal, Th.; Foglia, F.; Helm, L.; Merbach, A. E. *J. Am. Chem. Soc.* **1995**, *117*, 3790.
(33) Solera, J. A.; García, J.; Proietti, M. G. *Phys. Rev.* **1995**, *B51*, 2678.

phase functions was previously verified by using three reference rare-earth materials $NdAlO_3$, $NdCoO_3$, and $NdNiO_3$.[28] Notice that oxygen and nitrogen atoms have very similar backscattering amplitude and phase functions when calculated for the same distance. Consequently, only a small difference in the FT peak position (0.02 Å) and amplitude (about 10%) can be expected. Therefore, in the fitting procedure, these atoms will be distinguishable thanks to their characteristic distances in the $Gd(DTPA)^{2-}$ and $Gd(DOTA)^-$ complexes: Gd−O (R = 2.40 Å) and Gd−N (R = 2.65 Å).

Sharp double-electron excitations have been observed in the studied XAFS spectra. They are illustrated by two peaks with a width of several electronvolts located in the XAFS spectra about 6 $Å^{-1}$ (see Figure 2). In the case of the rare-earth L_3 edges, such signals have already been reported.[33−35] As was mentioned earlier, the presence of the double-excitation contribution modifies the fine structure beyond the absorption edge. This automatically leads to the distortion of the XAFS signal (and its FT) and, accordingly, increases the error in the determination of structural parameters. But our analysis showed that the influence of such effects on the FT was analogous to the effect of the steplike function; i.e., it produced a significant contribution only in the FT range above 5 Å.

Considering the signatures observed beyond the first shell, we paid attention to the MS effects which are known to modify the amplitudes and phases of the XAFS signals. The MS calculations (see Figures S2 and S3 (Supporting Information)) were performed using the FFEF6 code[29] for the $[Gd(DOTA)H_2O]^-$ anion with known crystallographic data.[8] We carried out the calculations with a cluster of 28 atoms within the 5 Å radius, taking into account all SS (single scattering) paths (28) and all MS (127) paths up to the third order and up to 6 Å.Thus, 127 paths, out of the total 148 paths, gave a contribution higher than 4% compared to the highest contribution of the shortest path Gd−O. The same MS calculations (see Figures S2 and S3) were performed for the $[Gd(DTPA)H_2O]^{2-}$ anion with known crystallographic data.[10,11]

First, we were interested in checking the correctness of the interatomic distances given by XRD for the complexes. Therefore, our top priority was to verify the good agreement between the frequency of the experimental and the calculated XAFS signals. Since thermal and structural disorders mainly influence the magnitude of the XAFS spectra, they were taken into account in an approximate way during the first step: the total SS and MS XAFS signals calculated were multiplied by an average thermal damping term $\exp(-2\sigma^2k^2)$ with σ^2 = 0.005 $Å^2$ for the crystalline complexes so that the signal amplitude nearly reached the experimental ones (see Figures S2 and S3).

Results and Discussion

The experimental XAFS spectra at room and low temperatures are presented in Figure 2 for the Gd L_3 edge of the $Gd(DOTA)^-$ and $Gd(DTPA)^{2-}$ complexes in the crystalline state, in comparison with the aqueous solutions at pH 1.5 (from 25 to 90 °C) and pH 7 (room temperature). The acidification of the $Gd(DTPA)^{2-}$ solutions (pH 1.5 to pH 0.2) leads to an obvious modification of the experimental XAFS signals related to the dissociation of this complex (see Figure 2c).

The experimental XAFS spectra were Fourier-transformed in the wavevector interval from 1 to 13 $Å^{-1}$, and their FT's are presented in Figure 3. As one can see, the XAFS signals differ for the $Gd(DOTA)^-$ and $Gd(DTPA)^{2-}$ complexes. Morever, the FT's of these two complexes differ more significantly from the FT of the Gd^{3+} ion in aqueous solutions.

The XAFS and FT's are close in the crystals and in the aqueous solutions at the different pH values from 1.5 to 7 and at various temperatures. We observed (see Figures 2 and 3) only a small increase of the DW factors. For the aqueous solutions, a greater DW value of 0.001 $Å^2$ was obtained. Note that, under these conditions, the dissociation of the complexes requires a matter of days: for example, $Gd(DOTA)^-$ shows a half-life of 85 days at pH 2 and more than 200 days at pH 5.[15] Obviously, during the limited synchrotron radiation beamtime, we could not observe these changes at pH 1.5−7.

On the other hand, the acidification and dissociation of the $Gd(DTPA)^{2-}$ solutions (pH 1.5 to pH 0.2) are evident in the experimental XAFS signals. At pH 0.2, the spectrum is identical to the one of the totally dissociated salt $GdCl_3$. For the intermediate pH values, each spectrum may be estimated by a linear combination of the extreme values (see Figure 3c): pH 0.15, 0% (completely dissociated $Gd(DOTA)^-$ complex); pH 0.75, 20%; pH 1.07, 35%; pH 1.2, 50%; pH 1.5, 100% (the percentage number is the complexation rate).

Previously it was concluded[15−17] that $Gd(DOTA)^-$ is the most inert lanthanide complex, relative to its very low dissociation rates. In fairly acidic media at pH 2 and lower, the negatively charged complexes can be effectively protonated and the assisted dissociation mechanism occurs.[16] Therefore, the XAFS results we obtained are in good agreement with these previous conclusions.

MS XAFS Analysis. During the first step of the data analysis, we tried to understand qualitatively the nature of the peaks in FT's in comparison with XRD data[8−11] and particularly the MS contributions. The MS calculated spectra using crystallographic data and experimental XAFS spectra are shown in Figure S2 for the $Gd(DOTA)^-$ and $Gd(DTPA)^{2-}$ complexes in the crystals. The modulus and imaginary parts of these FT's (see Figures S2 and S3) coincide very well. In comparison with the MS calculations, a decrease in the experimental peak amplitude due to thermal vibrations is clearly visible, especially for the peaks beyond the first one. Four main peaks are present in the FT's of the $Gd(DOTA)^-$ and $Gd(DTPA)^{2-}$ complexes (Figure S3): two peaks located at 1.6−2.5 Å with a maximum at 1.8 Å (label A), a smaller one at 2.3 Å (label B), another one located at 2.5−3.2 Å (labels C_1 and C_2) with a maximum at 3.0 Å, and, last, one located at 3.2−4.4 Å with a maximum at 3.8 Å (label D).

Additional MS and SS calculations for the clusters of different dimensions (starting from the single coordination shell cluster up to the cluster of 5 Å) allowed us to assign these different peaks. The first major peak (A) corresponds to the SS processes on the four carboxylate oxygen atoms (see Figure 1) forming the same side of the ring of the $Gd(DOTA)^-$ complex, on the five carboxylate oxygen atoms of $Gd(DTPA)^{2-}$ complex at the distance R(Gd−O) = 2.38 Å, and on one water oxygen (O_w) atom at the distance R(Gd−O_w) = 2.49 Å. The second peak (B) of the FT's is attributed to the SS processes on the four nitrogen atoms forming the other side of the ring of $Gd(DOTA)^-$ at the distance R(Gd−N) = 2.65 Å and on the three nitrogen atoms of $Gd(DTPA)^{2-}$ at the distance R(Gd−N) = 2.64 Å.

The next peaks (C_1 and C_2) of the FT's correspond mainly to the SS processes involving the second shell around gadolinium ions, formed by 16 (DOTA) and 14 (DTPA) carbon atoms located at 3.2−3.6 Å, which represents a contribution of about 30% (FEFF code notation). Its amplitude is significantly influenced by the DW factor. The first peak C_1 corresponds to a shorter distance of the carboxylic groups (Gd−O−C), and the second peak C_2 corresponds to a longer distance of the amino groups (Gd−N−C).

The MS calculations show that, above 3.0 Å, the MS signals start to contribute to the FT's (peak D). The first MS contribution originates from the four double scatterings (path length R_l = 3.45 Å) and four triple scatterings (Gd−O−C, R_l = 3.6 Å) in the four carboxylic groups. The next MS

(34) Purans, J.; Kuzmin, A.; Burattini, E. *Jpn. J. Appl. Phys.* **1993**, *32* (Suppl. 32-2), 64.
(35) Benazeth, S.; Tuilier, M. H.; Guittard, M. *Physica B* **1989**, *158*, 39.

contribution originates from the nine double (Gd−N−C, R_l = 3.8 Å) scatterings through the three nitrogen atoms. The MS effect in the first coordination shell of the gadolinium ion (O−Gd−N; O−Gd−O; N−Gd−N) gives a broad contribution (about 20 contributions with R_l = 3.8−4.2 Å) to the FT. Significant four double (R_l = 4.45 Å) and four triple (R_l = 4.5 Å) contributions originate from a quite linear chain (Gd--C═O) with four peripheral carboxylic groups.

Thus, we can conclude that the first peak (A) of FT's has a predominant oxygen atom origin and the second one (B) a mainly nitrogen atom origin, while the next peak (C_1) corresponds to the short distance (Gd−O−C_1) of the carboxylic groups and the second next peak (C_2) corresponds to the long distance (Gd−N−C_2) of the amino groups. Moreover, the MS signals are very sensitive to the distances and the angles between the atoms. Therefore, using the detailed MS analysis, we confirmed that the structure of the complexes is conserved up to 4.5 Å in the solutions studied and that the complexes have as strong a rigidity as in the crystals.

MS calculations (see Figure S1) were performed for the GdO_9 (three capped trigonal prism R = 2.41 Å) and GdO_8 (square antiprism R = 2.41 Å) clusters, which mimic the possible environment of Gd^{3+} ions in aqueous solutions. The first peak (A) of a FT's has an SS oxygen atom origin, while the second (C) and third ones (D) correspond to the double and triple MS effects in the first coordination shell of the gadolinium ion (O−Gd−O). They give the main contribution (about 36 tricapped prism double scattering contributions with R_l = 3.6 Å) to the FT. The next peak (E) can be assigned to the SS from the second hydration shell of gadolinium ions, which was previously detected by neutron scattering, and/or to high-order MS signals in the first hydration shell.

First Coordination Shell Fitting Results. For $Gd(DOTA)^-$ and $Gd(DTPA)^{2-}$ complexes, the best fit analysis of the XAFS signal was performed in the k range from 3.0 to 11.0 $Å^{-1}$ and in the 0.8−2.6 Å R range. Two contributions (Gd−O_{av}) and (Gd−N_{av}), related to the first shell, were singled out by the back FT in the intervals 0.8−2.6 Å (see Figure 3). Therefore a two-shell first model seems to be adequate as the first approximation. Moreover, the detailed analysis with the constant coordination numbers Gd−O(4) and Gd−N(4) shows that the signal of $Gd(DOTA)^-$ has a complex origin, and its description requires the XAFS signal related to the water molecule located in the first shell. Note that the values of the coordination numbers of Gd−O_{av}, Gd−O_w, and Gd−N_{av} did not vary during the three shell fitting procedures.

Usually, the maximum number of fitting parameters is limited by the number of independent data points $N_{ind} \cong 2\,\Delta k\,\Delta R/\pi + 2$ where Δk and ΔR are respectively the widths in the k and R spaces used in the fit.[26] In the case of the first coordination shell, N_{ind} is about 12 (Δk = 9 $Å^{-1}$ and ΔR = 1.8 Å). Thus, if we take two fitting parameters per contribution, the maximum number of contributions which can be used is 6. We used two (Gd−O_{av} and Gd−N_{av}) and three (Gd−O_{av}, Gd−O_w, and Gd−N_{av}) contribution models with four and six possible varying parameters. Finally, the fitting parameters for each contribution were distances and DW factors.

We found that the use of the two- and three-shell models agreed well with experiment for $Gd(DOTA)^-$. On the basis of the two contribution fitting parameters, the radial distribution function (RDF) can be reconstructed according to the equation of the sum of Gaussian distributions.[25,28] This graphical representation (see Figure 4) is useful since it takes into account not only the coordination numbers and the peak positions but also the DW factor values (static and dynamic part) and overlaps from the different shell contributions. In the following section, we will compare our results with the local environment around gadolinium ions in crystals. The results of the fitting procedures are gathered in the Table 1.

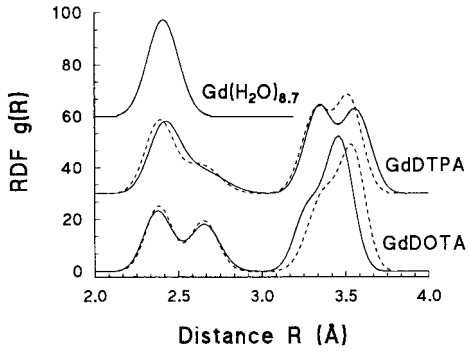

Figure 4. Reconstructed RDF's of the first and second coordination shells of the $Gd(DOTA)^-$ and $Gd(DTPA)^{2-}$ complexes in the crystals at RT, obtained from XAFS data (full lines) and based on the XRD data (dashed lines). The RDF for the Gd^{3+} ions in aqueous solution is shown as well.

Table 1. First Coordination Shell Structural Data Obtained from the Best-Fit Analysis of the Gd Complexes in the Crystalline State (cr) and Solutions (sol)[a]

	Gd−O_{av} and Gd−O_w			Gd−N_{av}			
state	N_1	R_1 (Å)	σ_1^2 (Å^2)	N_2	R_2 (Å)	σ_2^2 (Å^2)	ϵ ($\times 10^{-3}$)
			$Gd(DTPA)^-$				
cr RT[b]	$5O_{av}$	2.404		$3N_{av}$	2.640		
cr RT[b]	O_w	2.490					
cr RT[b]	$5O_{av} + O_w$	2.418					
cr LT	$5O_{av} + O_w$	2.382	0.0051	$3N_{av}$	2.601	0.0141	2.3
cr RT	$5O_{av} + O_w$	2.389	0.0073	$3N_{av}$	2.638	0.0115	1.5
sol 25 °C	$5O_{av} + O_w$	2.394	0.0058	$3N_{av}$	2.644	0.0054	1.8
sol 50 °C	$5O_{av} + O_w$	2.400	0.0072	$3N_{av}$	2.652	0.0081	1.8
sol 80 °C	$5O_{av} + O_w$	2.404	0.0067	$3N_{av}$	2.678	0.0064	1.8
			$Gd(DOTA)^{2-}$				
cr RT[c]	$4O_{av}$	2.364		$4N_{av}$	2.662		
cr RT[c]	O_w	2.447					
cr RT[c]	$4O_{av} + O_w$	2.381					
cr RT	$4O_{av} + O_w$	2.384	0.0063	$4N_{av}$	2.653	0.0067	2.1
sol 25 °C	$4O_{av} + O_w$	2.382	0.0065	$4N_{av}$	2.640	0.0070	2.6
sol 49 °C	$4O_{av} + O_w$	2.385	0.0064	$4N_{av}$	2.646	0.0067	2.1
sol 74 °C	$4O_{av} + O_w$	2.388	0.0068	$4N_{av}$	2.650	0.0069	1.9
sol 87 °C	$4O_{av} + O_w$	2.390	0.0074	$4N_{av}$	2.650	0.0072	1.3
sol pH 7	$4O_{av} + O_w$	2.401	0.0089	$4N_{av}$	2.681	0.0054	1.0
			Ln^{3+} in Aqueous Solution				
Sm^{3+} N[d]	8.5	2.46					
Eu^{3+} E[e]	12.0	2.41	0.007				
Gd^{3+} E[f]	7.6	2.43	0.004				
Gd^{3+} X[g]	8.0	2.37					
Gd^{3+}	8.7	2.41	0.008				

[a] N_i is the number of atoms located in the ith shell at the distance R from the Gd, σ^2 is the DW factor, and ϵ is the fitting error. Absolute errors are ±0.01 Å on R and ±0.002 Å^2 on σ^2. This error bar is lowered when we compare different measurements to ±0.003 Å on R and ±0.001 Å^2 on σ^2. [b] From XRD data of ref 10. [c] From XRD data of ref 8. [d] From neutron (N) scattering data of ref 30. [e] From XAFS (E) data of ref 33. [f] From XAFS (E) data of ref 24. [g] From XRD (X) data of ref 36.

The results of the fitting procedures are as follows: in the crystalline and aqueous solutions, the gadolinium ions in the complex $Gd(DOTA)^-$ are strongly bonded to the four carboxylate oxygen atoms ((Gd−O_{av}) distance close to 2.38 ± 0.01 Å, with the small DW factor 0.006 ± 0.002 Å^2) and to the four

nitrogen atoms ((Gd−N_{av}) distance close to 2.65 ± 0.02 Å, with the DW factor about 0.006 ± 0.003 Å^2). Moreover, the results of the three-contribution model have shown that the oxygen atom of the water molecule is at about a (Gd−O_w) distance of 2.46 ± 0.05 Å, with a DW factor equal to 0.012 ± 0.005 Å^2.

Concerning the complex Gd(DTPA)$^{2-}$, the gadolinium ions are strongly bonded to the five carbonyl oxygen atoms (R(Gd−O_{av}) close to 2.39 ± 0.01 Å, with a DW factor 0.007 ± 0.002 Å^2) and to the three nitrogen atoms (R(Gd−N_{av}) close to 2.64 ± 0.02 Å, with a DW factor equal to 0.011 ± 0.003 Å^2 in crystals and equal to 0.006 ± 0.002 Å^2 in solutions). The water molecule is at about the R(Gd−O_w) distance 2.47 ± 0.05 Å, with the DW factor 0.018 ± 0.005 Å^2. The fitting error is calculated by eq 2 in the ref 28.

The experimental radial distribution functions (RDF's) obtained from XAFS structural parameters (see method in ref 28, eq 3) were also compared with the calculated ones for the Gd ions in the crystallographic environment. They were reconstructed on the basis of the XRD data and the DW factors obtained from XAFS. Through this graphical representation the structural disorder (set of distances) and the thermal (vibrational) disorder are qualitatively taken into account and presented in Figure 4. One can see that RDF's obtained by two different methods coincide well. The first double peak corresponds to (Gd−O_{av}), (Gd−O_w), and (Gd−N_{av}) distances. The second peak is quite separated for the Gd(DOTA)$^-$ complex and less resolved for the Gd(DTPA)$^{2-}$ complex due to the different structural (set of distances) and thermal disorders.

The first shell distances obtained in the Gd(DOTA)$^-$ complex (solid state and solutions) agree particularly well with the previous ones obtained by an XRD technique for the crystals at RT.[8,9] But in the case of the Gd(DTPA)$^{2-}$ complex, the coincidence was partial[10] (see Table 1 and Figure 4). Therefore, the complexes conserve the same characteristic distances and geometry in the solution as in the solid state, which influences the stability and the rate of the acid-assisted dissociation of the Gd complexes through the influence of the well-known factors metal ion size, charge density, and rigidity.[16]

Concerning the aqueous solutions, the first shell structural parameters we obtained correspond well, especially for Gd(DOTA)$^-$, with previous ones resulting from neutron scattering experiments[30,31] and molecular dynamics simulations.[32] The discrepancy is much more significant when we compare our results with those of previous XAFS analyses.[24,33]

These previous results from XAFS measurements of rare-earth ions in solutions are an example of the controversy. The more recent XAFS structural results[24] concerning the rare-earth ions in 2 M solutions were obtained by Yamaguchi et al. They determined a coordination number (CN) of 9 for Nd^{3+}, a CN between 9 and 8 for Sm^{3+} and Eu^{3+}, and a constant CN for the heavier elements: 9.5 (Nd^{3+}), 7.6 (Gd^{3+}), 7.7 (Lu^{3+}), with an estimated error of ±0.5. These values agree with the neutron diffraction measurements[30,31] and MD simulations,[32] if we take into account the approximated theoretical phase and amplitude calculations used by the authors. On the other hand, Solera et al.[33] recently extensively investigated the XAFS and multielectron excitation occurring at the L edges of rare-earth ions in low-concentration solutions (0.05, 0.1, and 0.2 M) and concluded that the rare-earth ions are always surrounded by 12 water molecules with a cubooctahedral symmetry, which disagrees with the neutron diffraction measurements[30,31] and MD simulations.[32] Concerning the distance in the first coordination shell, a better agreement has been obtained from these two XAFS[24,33] studies: the distance is found to decrease from 2.56 Å for La^{3+} down to 2.32 Å for Tm^{3+}. Considering now the DW factor, the values obtained by these two groups of authors differ significantly; for example, for the Eu^{3+} ions, Solera et al.[33] obtained 0.0075 ± 0.003 Å^2 but Yamaguchi et al.[24] obtained 0.0055 Å^2.

Table 2. Second Coordination Shell Structural Data Obtained from the Best-Fit Analysis of the Gd Complexes in the Crystalline (cr) State and Solutions (sol)[a]

	Gd−C_1			Gd−C_2			
state	N_1	R_1 (Å)	σ_1^2 (Å^2)	N_2	R_2 (Å)	σ_2^2 (Å^2)	ϵ (×10^{-4})
			Gd(DTPA)$^{2-}$				
cr RT X[b]	7	3.347		7	3.556		
cr LT	7	3.352	0.0043	7	3.538	0.0048	5.8
cr RT	7	3.327	0.0074	7	3.525	0.0060	1.7
sol 25 °C	7	3.372	0.0075	7	3.559	0.0081	3.2
sol 50 °C	7	3.369	0.0069	7	3.562	0.0066	2.7
sol 80 °C	7	3.363	0.0079	7	3.560	0.0075	2.1
sol pH 7	7	3.366	0.0045	7	3.540	0.0047	2.6
			Gd(DOTA)$^-$				
cr RT X[c]	8	3.290		8	3.460		
cr LT	7	3.369	0.0096	8	3.531	0.0058	5.4
cr RT	7	3.371	0.0089	8	3.548	0.0054	4.1
sol 25 °C	7	3.354	0.0076	8	3.540	0.0065	6.5
sol 49 °C	7	3.360	0.0081	8	3.539	0.0049	4.1
sol 74 °C	7	3.365	0.0075	8	3.547	0.0050	4.2
sol 87 °C	7	3.361	0.0079	8	3.542	0.0049	3.7
sol pH 7	7	3.368	0.0072	8	3.537	0.0045	6.3

[a] N_i is the number of atoms located in the ith shell at the distance R from the Gd, σ^2 is the DW factor, and ϵ is the fitting error. Absolute errors are ±0.01 Å on R and ±0.002 Å^2 on σ^2. This error bar is lowered when we compare different measurements to ±0.003 Å on R and ±0.001 Å^2 on σ^2. [b] From XRD data of ref 11. [c] From XRD data of ref 8.

We may interpret our experimental XAFS data, measured at the L edges of Gd^{3+} ions in aqueous solutions, as composed of a two-frequency signal: a dominant low-frequency signal from atoms located in the first coordination shell and a weak higher-frequency signal, attributed to the multiple-scattering effects and to the second hydration shell. The existence of the outer hydration shells around the Gd^{3+} ions in the aqueous solutions was previously intensively investigated and confirmed by neutron diffraction[30,31] and MD simulations.[32] Its contribution consists of a quite broad second hydration shell, formed by nearly 16−18 water molecules, located around Ln^{3+} ions at the mean distance R(Ln−OH_2) = 3.7−5.4 Å with a full width at half-height of the first peak about 0.24−0.31 Å. From our point of view, the second high-frequency component of the XAFS signal is dominated by the multiple-scattering signal generated within the first coordination shell of tricapped trigonal prism GdO_9. We have observed that the signals from the coordination shells, located beyond the first one, are strongly damped due to high static and thermal disorder while the multiple-scattering signal from the first coordination shell produces a significant contribution to the total XAFS and is in good agreement with the high-frequency component discussed above.

Second Coordination Shell Fitting Results. As previously explained, the C_1 and C_2 peaks of the FT's mainly correspond to SS from the Gd surrounding second shell, formed by 14 (for DTPA) or 16 (for DOTA) carbon atoms located at 3.23−3.52 Å. In the case of the second coordination shell, the maximum number of fitting parameters N_{ind} is about 9 (Δk = 8 Å^{-1} and ΔR = 1.2 Å). Thus, if we also take two fitting parameters per contribution, the maximum number of contributions which can be used is 4. We used two SS contributions Gd−C_1 (C_1 from the carboxylic group) and Gd−C_2 (C_2 from the amino group)

with four varying parameters, and the fitted parameters for each contribution were distances and DW factors.

The second shell distances obtained in the $Gd(DOTA)^-$ and $Gd(DTPA)^{2-}$ complexes (solid state and solutions) partially agree with those previously deduced from XRD technique in the crystals at RT(see Table 2 and Figure 4).[8,11]

Conclusions

We presented a detailed X-ray absorption spectroscopy study of the local structure around the Gd^{3+} ions in the complexes $Gd(DTPA)^{2-}$ and $Gd(DOTA)^-$ as crystals and in aqueous solutions. We found that the complexes are very rigid (small DW factors) and that the gadolinium local environment in these complexes is conserved up to 4.5 Å in aqueous solutions with pH 7 and is still so when the pH decreases to 1.5. The XAFS signals differed for the $Gd(DOTA)^-$ and $Gd(DTPA)^{2-}$ complexes, but for each of these complexes, we observed no significant change in the two different cases: crystalline state and aqueous solutions at pH 1.5−7. The slight changes with temperature are related to a small increase in the Debye−Waller (DW) factors. The acidification of the $Gd(DTPA)^{2-}$ solutions (pH 1.5 to pH 0.2) led to an obvious modification of the experimental XAFS signals related to the dissociation of this complex.

The experimental FT's of the complexes studied as crystals and in aqueous solutions can easily be explained by MS calculations with structural parameters close to those known from crystallographic data. These values for the first ($Gd-O_{av}$ and $Gd-N_{av}$) and second ($Gd-C_1$ and $Gd-C_2$) shells agreed with those obtained by X-ray diffraction techniques.[8−11] The obtained first shell distances for the $Gd(DOTA)^-$ complex (solid state and solutions) are in good agreement with the ones previously obtained by the XRD technique for the crystalline form at RT. For $Gd(DTPA)^{2-}$, the agreement is at a lower level.

Our XAFS study also supplies additional information about the complex rigidity and dynamics provided by the characteristic DW factor values. Therefore XAFS spectroscopy, which has not yet been used to study gadolinium $DOTA^-$ and $DTPA^-$ like complexes, appears to be a powerful method to obtain structural and vibrational information on aqueous solution forms of rare-earth complexes. The RDF's obtained from this method could be compared directly with the RDF's calculated with molecular dynamics simulations.[37,38]

Acknowledgment. J.P. thanks Prof. C. Souleau, Laboratoire de Chimie Bioinorganique, Centre pharmaceutique, Châtenay-Malabry, Universite-Paris-Sud, for his great help during this work. Special thanks are expressed to the General Council of Essonne Department (France) for the financial support of J.P. The authors are grateful to the LURE laboratory for their hospitality and express special thanks to Professor A. M. Marty for correcting the English language in this paper.

Supporting Information Available: Figure S1, showing the XAFS spectra and FT's (modulus and imaginary parts) of the Gd^{3+} ion in the aqueous solution (experimental spectra at pH 7.0 and RT and MS calculated spectra of the tricapped prism and square antiprism), Figure S2, showing the XAFS, and Figure S3, showing the FT's (modulus and imaginary parts), demonstrating the comparison of the experimental XAFS spectra and the MS calculated spectra of the $Gd(DOTA)^-$ and $Gd(DTPA)^{2-}$ complexes in the crystalline state (7 pages). Ordering information is given on any current masthead page.

IC9707321

(36) Steele, M. L.; Wertz, D. L. *J. Am. Chem. Soc*. **1996**, *98*, 4424.
(37) Fossheim, R.; Dugstad, H.; Dalh, S. G. *J. Med. Chem*. **1991**, *34*, 819.
(38) Foosheim, R.; Dahl, S. G. *Acta Chem. Scand*. **1990**, *44*, 698.